

Clock synchronization with correlated photons

Christopher Spiess* and Meritxell Cabrejo Ponce

Friedrich Schiller University Jena, Fürstengraben 1, 07743 Jena

Fraunhofer Institute for Applied Optics and Precision Engineering, Albert-Einstein-Strasse 7, 07745 Jena and

Max Planck School of Photonics, Albert-Einstein-Str. 7, 07745 Jena, Germany

Sebastian Töpfer and Daniel Rieländer

Fraunhofer Institute for Applied Optics and Precision Engineering, Albert-Einstein-Strasse 7, 07745 Jena

Sakshi Sharma

Friedrich Schiller University Jena, Fürstengraben 1, 07743 Jena and

Fraunhofer Institute for Applied Optics and Precision Engineering, Albert-Einstein-Strasse 7, 07745 Jena

Fabian Steinlechner†

Fraunhofer Institute for Applied Optics and Precision Engineering, Albert-Einstein-Strasse 7, 07745 Jena and

Friedrich Schiller University Jena, Abbe Center of Photonics, Albert-Einstein-Strasse 6, 07745 Jena

(Dated: July 4, 2022)

Event synchronisation is a ubiquitous task, with applications ranging from 5G technology to industrial automation and smart power grids. The emergence of quantum communication networks will further increase the demands for synchronisation in optical and electronic domains, thus incurring a significant resource overhead, e.g. through the use of ultra-stable clocks or additional synchronisation lasers. Here we show how temporal correlations of energy-time entangled photons may be harnessed for synchronisation in quantum networks. We achieve stable synchronisation jitter < 50 ps with as few as 36 correlated detection events per 100 ms and demonstrate feasibility in realistic high-loss link scenarios. In contrast to previous work, this is accomplished without any external timing reference and only simple crystal oscillators. Our approach replaces the optical and electronic transmission of timing signals with classical communication and computer-aided post-processing. It can be easily integrated into a wide range of quantum communication networks and could pave the way to future applications in entanglement-based secure time transmission.

I. INTRODUCTION

Secure transmission of information and reliable event synchronisation are key requirements in critical infrastructures [1, 2], especially in power grids [3], financial networks [4] or cloud database services [5]. With regards to information security, quantum key distribution (QKD) offers the unique proposition of encryption keys whose confidentiality can be lower bounded from the very laws of physics [6–9]. Quantum communication is thus poised to becoming a backbone of secure information infrastructures, with networks of many hundreds of fibre links established, and integration of ground-space relays over more than 1,000 kilometres already underway [10].

Quantum communication networks, which involve tight timing budgets in the optical and electronic domains, are also a prime example for the need for accurate synchronisation of remote parties. In classical communication networks, the Network Time Protocol (NTP) achieves synchronization with accuracy down to milliseconds [11] or nanoseconds through the Global Navigation Satellite System (GNSS) [12]. High-bit-rate QKD systems however operate at the level of picosecond timescales, and inevitably call for even better synchronization [13]. In state-of-the-art QKD systems this is typically achieved by

auxiliary pulsed lasers [10, 14, 15] or stable references [16], like Rubidium clocks [17–19] or GNSS [20, 21]. Specialized classical infrastructure together with novel implementation of the high-precision White Rabbit protocol [22] may reach sufficient performance as well [23]. All together, these auxiliary components create a significant resource overhead that reduces scalability [24] or applicability in space due to tight power consumption and weight constraints [25, 26]. Moreover, much like the case in classical telecommunication networks, these requirements are likely to increase further when considering advanced network protocols, e.g., quantum teleportation [27, 28] and entanglement swapping [29, 30].

Quantum clock synchronization protocols have been proposed to tackle synchronizing distant clocks [31–33] in multi-partite network settings [34, 35] and with quantum-enhancement beyond the possibilities of classical physics [36]. To this end, investigations over the last years have focused on exploitation of the temporal correlations of time-energy entangled photons created via parametric down conversion [37–40]. When photon pairs originate from common creation event, this gives rise to a narrow correlation peak in their arrival time at remote receivers. By using the correlation peak location [41, 42], it is surprisingly simple to extract the time and frequency differences between remote clocks. The recent past has seen further advancement with experiments achieving exceptionally high precision with respect to a common frequency reference [43]: 600 fs with correlated photons [37], or down to 60 fs using Hong-Ou mandel interference [38–40]. In

* christopher.spiess@iof.fraunhofer.de

† fabian.steinlechner@iof.fraunhofer.de

deployed long-distance links, synchronization jitters as low as a few tens of picosecond have been demonstrated using ultra-precise Rubidium clocks [18, 21, 44]. Without atomic frequency references, the timing jitter attainable is orders of magnitude higher (e.g., the frequency offset for standard crystal oscillators may be up to 8 orders of magnitude higher[45, 46]). This frequency difference results in a temporal drift of the correlation peak and makes it impossible to find the initial timing offset for synchronization, thus limiting application of correlated photons [42]. The added complexity of Rubidium clocks, GPS-disciplined clocks or other common references has long been a necessary requirement for deployed long-distance and high-bit rate quantum communication systems in real operational conditions [16, 18, 19, 21].

In this article, we build on the ground-breaking work of Ho[42] and Valencia[41] and establish the feasibility of picosecond-level synchronization with photon pairs for realistic link scenarios. Unlike state-of-the-art field experiments, which employ active electro-optic modulation [47–49], we accomplish this in post-processing without any requirement for auxiliary hardware. Our approach bases on predictive estimation of clock frequency difference and compensation of the dispersion of correlation peaks. By efficient tracking of the correlation peak position during the communication session we correct for residual clock instabilities and achieve synchronization jitters < 50 ps with correlation rates as low as 360 ± 70 correlation events per second. Notably, these values are comparable to $30 - 50$ ps jitters reported for uncompensated systems that employ GPS-disciplined Rubidium clocks [18, 21]. Finally, we study the effect of limited signal to noise ratio and establish the feasibility in real high-loss link conditions. The results of our proof of concept experiment show that time-correlated photon pairs are a valuable resource for timing synchronization with minimal hardware overhead, not only for laboratory experiments, but also for deployed QKD systems in high-loss link scenarios. Our approach provides a simple way of enhancing the timing resolution in distributed quantum information processing tasks and may also indicate new directions towards fully harnessing time-frequency entanglement in quantum sensing and quantum information processing networks. The method for software-based synchronization in post-processing can be implemented straightforwardly in state of the art quantum key distribution systems and pave the way towards tomorrow's quantum networks [50], including secure time transfer [51, 52].

II. RESULTS

The workflow for synchronization of remote parties consists of four main steps from coarse millisecond timing down to regions of picosecond or smaller (Fig. 1a). At its core lies a source that generates two entangled photons (signal and idler) with intrinsic timing correlations. The distributed photons operate as mediator between distant parties, providing the opportunity to remotely

recover timing relations from correlation events (Fig. 1a). The photon pair timing accuracy can be as high as femtoseconds [53], but special care has to be taken for the other system components that lower the precision. The first part of successful synchronization with correlated photons is temporal alignment of data packages at the photon receiver (Fig. 1b). Time taggers take track of the photon's arrival time and store them on computer in data packages with size and acquisition time of approximately 100 ms. Coarse millisecond synchronization makes sure that packages are matched and carry correlated photons by classical network pinging through the network time protocol [11] - this procedure is not part of the paper. Second, the precise time difference between master and slave, i.e. timing offset, is calculated by means of time tags of matched data packages, via a Fast Fourier Transformation (FFT) convolution [42]. The ability to recover the correlation peak is essential for synchronization and is strongly influenced by the characteristics of the remote clocks. The following two terms describe clock's behavior [45]: clock skew as the frequency difference between master and slave, and clock drift as the first derivative with respect to time of the skew. High precision of clocks is indicated by small skew and highly stable clocks will have low clock drifts. Strong clock skews are indicated by high drifts of the correlation peak in time, resulting in significant peak spreading while time passes by, which renders clock recovery difficult - if not impossible. Coarse skew compensation allows to identify the correlation peak with timing offset precision < 100 ns even for strong skews. Third, we fine-tune the clock skew through calculating the correlation peak over a computation-efficient Start-Stop method [54–56]. In summary, we estimate the timing offset in step 2 and find the clock skew with high precision in step 3. These are the requirements to start the quantum communication session. In the course of a long communication session, the frequency of unstable clocks changes unpredictable, introducing errors of the previous estimation and follows in an enormous increase of the total system jitter. Only live tracking of the correlation peak during the communication session and fast feedback loops in step 4 can catch up with fast variations of the clock skew.

With the basic workflow established, we now consider the challenge associated with real link scenarios with low signal to noise ratio and simultaneously high clock skew during initialization. The start sequence for a communication session is recognized by measuring the timing offset between Alice and Bob. Accumulation of simultaneous photon detection events from matched data packages results in a correlation peak located at the timing offset between two communicating parties. The offset can only be found if the peak was identified under a noisy background. For that, we introduce the statistical significance as the peak height normalized to the noisy background standard deviation[42]. Strong spread of the correlation peak in time reduces the significance. Important part of the total root-mean-squared (RMS) jitter is synchronization jitter σ_{sync} that increases with acquisition time T_A and uncorrected clock skew Δu ,

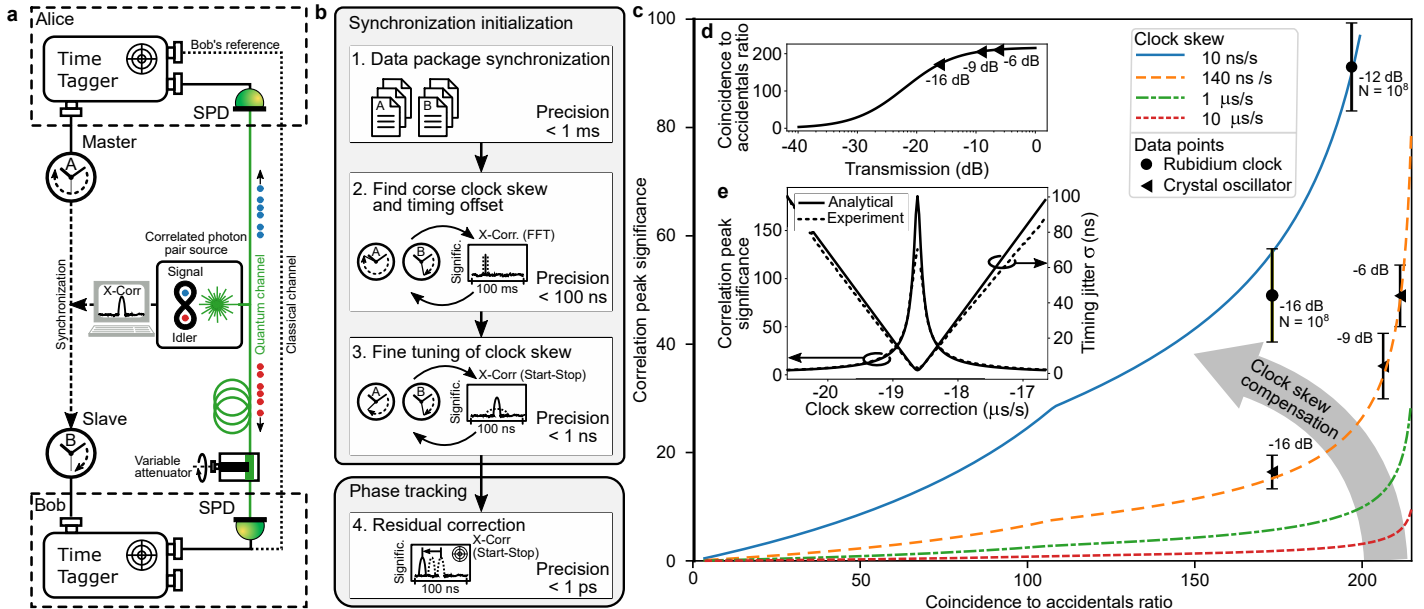


FIG. 1. Schematic synchronization workflow and calculation of timing offset with correlated photons. **a** Time-correlated photons, detected on single photon detectors (SPD), act as mediator to synchronize the master and slave clock of two communicating parties Alice and Bob through cross-correlation. The clocks may be the time tagger's internal Quartz crystal oscillators or external Rubidium clocks. The synchronization performance is compared with a local reference from Bob for varying quantum channel attenuation. **b** Steps for synchronization include package synchronization, timing offset calculation, clock skew estimation and correlation peak tracking over Fast-Fourier Transformation (FFT) or Start-Stop method-based cross-correlations. **c** Estimation of correlation peak significance under different coincidence-to-accidentals ratios (loss) and clock skews Δu . The experimental data points base on initial lossless rates of $R_A = 200$ kcps, $R_B = 800$ kcps, $R_C = 14$ kcps and maximum number of cross-correlation points $N = 10^8$. Error bars indicate standard deviation after slight variation of bin sizes. **d** Coincidence-to-accidentals ratio depending on the transmission from Alice to Bob. **e** The ratio of peak height to background standard deviation (significance) increases and the correlation peak spread reduces for correctly compensated clock skew.

$$\sigma_{\text{sync}} = \frac{1}{2} \Delta u T_A. \quad (1)$$

Any skew reduces the peak height, as described in [42] and will lower the probability to find it (Fig. 1c). The same applies to the signal to noise ratio $\text{CAR}(T) = (r_C T) / (2r_A r_B T \sigma + r_{\text{dark}})$ that reduces with increased losses (Fig. 1d) and eventually impacts the correlation peak height (see Methods IV A 1). Significance of barely 10 may be reached at experimentally relevant strong clock skews beyond $10 \mu\text{s}/\text{s}$. To counteract this, we introduce compensation of the skew, so that time tags on Bob's side $b(t)$ are corrected to $b_{\text{corr}}(t)$,

$$b_{\text{corr}}(t) = b(t) - \Delta u_{\text{corr}} [b(t) - b(t_0)]. \quad (2)$$

For different values of corrections Δu_{corr} we calculate the cross-correlation under the constraint of computation efforts, limiting us to approximately 280 cross-correlations. That corresponds to a step size of $0.14 \mu\text{s}/\text{s}$ in the clock skew search window from -20 to $+20 \mu\text{s}/\text{s}$, in consequence realizing an effective clock skew after compensation of $< 0.14 \mu\text{s}/\text{s}$. It allows for increasing the significance drastically, as we go from the red curve to orange in Fig. 1c. Optimum clock skew is indicated by maximum significance of the correlation peak in the search window (Fig. 1e). The correlation peak is fit by a stretched

Gaussian function and the timing jitter is calculated. The linear decrease of jitter, as well as the peak significance increase, matches very well with simulation and reaches a maximum significance of 160 (see Methods IV A 1). The analytical significance in addition matches different loss values after skew compensation in experiment (data points in Fig. 1c). Rubidium clocks have much lower skew and grant access to higher significance's (blue curve in 1c). In general, the correlation peak is easy to recover, even under real link scenarios with losses of 16 dB and strong clock skew of $18.5 \mu\text{s}/\text{s}$. After estimation of the start sequence, i.e. the timing offset and the intermediate step of clock skew fine tuning to limit the synchronization jitter (see Methods IV B), we are finally ready to start with the communication session.

Weak stability of clocks result in strong changes of the synchronization jitter over the communication session, due to time dependent deviations from the previously calculated optimum skew. This paragraph explains live tracking of the correlation peak in time intervals < 1 second to correct for fast changes of skew in real time. The correlation peak location is a reliable indicator of the instantaneous clock skew. Any constant residual clock skew results in change of the correlation peak location with constant speed, whereas acceleration is indicator of varied clock skew and thus apparent clock drift. In previous synchronization steps we estimated precisely the clock skew that would provide fixed correlation peak locations. However,

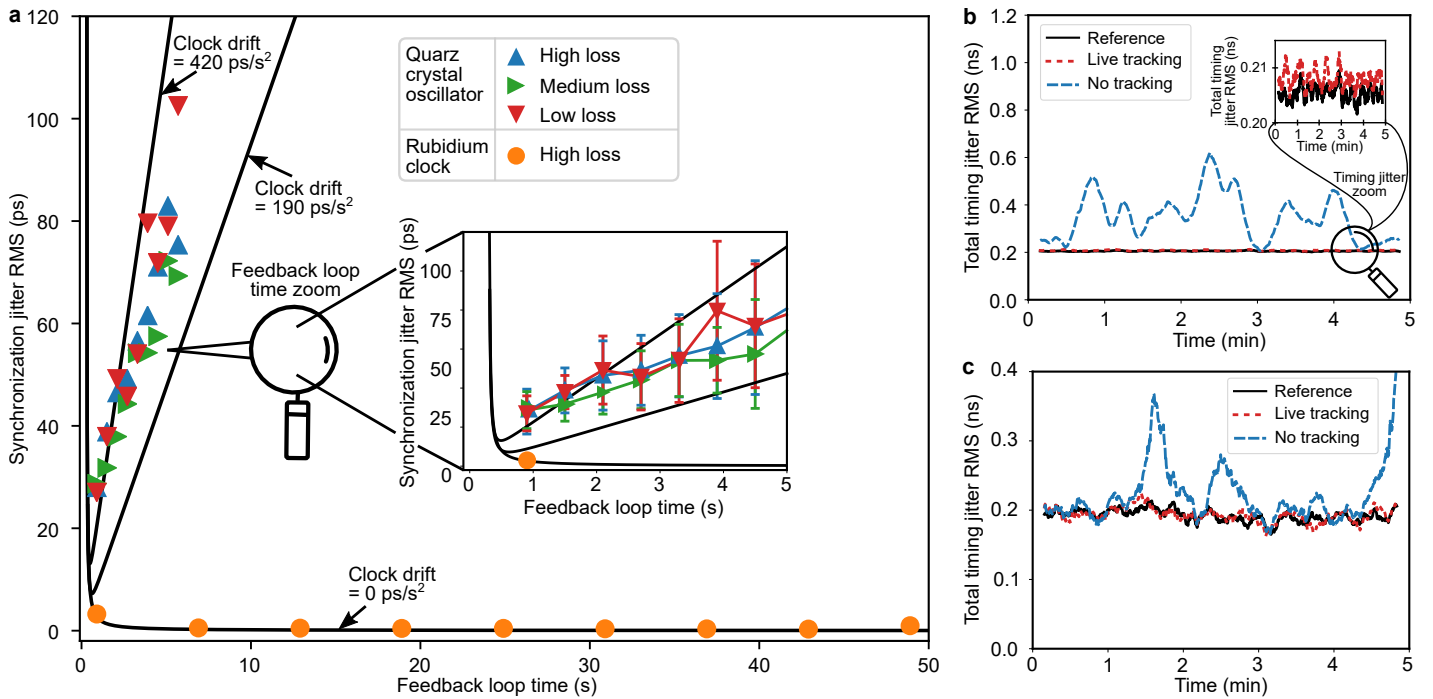


FIG. 2. **Synchronization jitter limits and experimental long term measurement of jitter** **a** Black lines represent root-mean-squared (RMS) jitter limits of theory for coincidence rate R_C of 1200 cps and variation of clock drift. Measurements are indicated by markers for high loss ($R_C \approx 1,200$ cps), medium losses ($R_C \approx 8,000$ cps) and low loss regime ($R_C \approx 24,000$ cps). The inset represents error bars corresponding to the standard deviation during 5-min measurement. **b-c** Comparison of total system jitter with correlated photons and reference for 100 ms data package size and 600 ms feedback loop time. The figure **b** refers to low loss regime with 1000 correlation events per data package and figure **c** to high loss regime with 36 correlation events according to Table I

as the clock drifts, the location will change and directly shows existing clock drift. The location is continuously tracked, and the skew afterwards adapted by the peak displacement over passed time. The location can be measured with precision down to an uncertainty given in [42], due to limited number of correlation events and translates to an erroneous clock skew and timing jitter, correspondingly (see Methods IV A 2 and IV C). The other jitter contribution comes from the clock drift, being the first temporal derivative of the clock skew. Depending on the feedback loop time will either the measurement jitter or jitters from drifting clocks dominate (Fig. 2a). High times for the feedback loop means that fast changing clock skews can not be compensated early enough and result in higher clock drift jitter. However, especially in high loss domain will small feedback loops give rise to substantial measurement errors, as the calculated clock skew scales with the feedback time. The relations are confirmed in experiment from measuring the total jitter with respect to the reference without synchronization jitter on the same data set. Important to note is that the synchronization jitter is independent of the loss regime for bigger feedback loops, due to marginal influence from measurement jitters. As the jitter of Rubidium clocks is < 1 ps over an acquisition time of 100 ms (see Methods IV C), it is difficult to measure directly. Here we derived it through the residual change of correlation peak timing offset. Figure 2b compares the total timing jitter with and without live tracking to Bob's reference that indicates zero synchronization jitter (see and Table I and Methods IV D). The acquisition time is 100 ms and feed-

back loop time 600 ms. Without live tracking, the residual timing jitter increases from 200 ps to almost 700 ps, due to time-dependent skew (i.e. existing clock drift) that could not be foreseen by synchronization initialization (steps 1-3). Over a time window of 5 min we find maximum clock skew variation up to ± 11 ns/s that show the importance of live correcting these residual drifts (see Methods IV E). Applying the live tracking algorithms clearly reduces the timing jitter to a noisy background level. To better see deviations between the reference jitter and our synchronization method, we plot data by a moving mean over 10 seconds. The reference jitter RMS calculates as 205.3 ± 1.3 ps and with live tracking 208.3 ± 1.7 ps over 5 min. The synchronization jitter from residuals is 34 ± 8 ps over 10 seconds of moving mean. Figure 2c presents stable synchronization down to RMS jitters of 48 ± 19 ps for much lower rates (Table I). Note that the correlation events per data package of 100 ms is only 36, being sufficient for finding the timing offset under strong skew and tracking of clock drift.

III. DISCUSSION

Clock skew compensation and higher order live tracking enables going beyond state-of-the art and replace highly stable references in real-life scenarios. We could show that 36 correlation events in 100 ms data packages are sufficient to establish and keep a synchronized quantum communication session to an average precision of < 48 ps over time scales of 5 minutes. Equation 10 in Methods IV A 1 and

TABLE I. Residual synchronization jitter after clock drift live correction for different transmission losses. Synchronization jitter in [18, 21] is estimated from timing offset variation.

Parameter	a Low loss	b High loss	c Steinlechner2017[18]	d Ecker2021 [21]
Rubidium clock	No	No	Yes	Yes
Count rate Alice (kcps)	271 ± 20	189 ± 21	400	13,300
Count rate Bob (kcps)	283 ± 22	10 ± 1	100	10
Correlation event rate (cps)	$10,300 \pm 800$	360 ± 70	20,000	> 300
Synchronization jitter RMS (ps)	34 ± 8	48 ± 19	≈ 33	≈ 50
Clock drift RMS (ps/s ²)	320	320	-	-

reference [42] predicts that sufficient significance > 10 can only be achieved by clock skews < 19 ns/s under high loss rates (Table Ib). Finding the initial timing offset for synchronization is predicted to fail already, as our clock skew is much greater and amounts to approximately 18.5 μ s/s. Here we demonstrated successful synchronization, due to compensation down to an effective skew of smaller 14 ns over 100 ms data package size that enables significance > 10 . Similar conclusions apply to typical quantum communication schemes (Table Ic), requiring clock skews of only < 50 ns/s that can easily be achieved with our scheme. High number of correlations events $R_C = 20$ kcps would also enable small synchronization jitter with short feedback loops (see Methods IV A 1, Fig. 2a). Intrinsic timing relations of correlated photons clearly have the potential to replace bulky external high-precision synchronization schemes and move resources from hardware to software.

Finding the timing offset is crucial to start communication, but low signal to noise ratio will reduce the correlation peak significance. Especially high-loss scenarios > 46.9 dB[21] (Table Id) call for clock skews on the order of 2 ns/s. Within the presented search window -20 μ s/s to $+20$ μ s/s it is impossible to find compensation down to required accuracy < 2 ns/s, due to very high computation times. In addition, for extended computation time it may be necessary to re-synchronize upcoming data packages via NTP, as correlated timetags drift in different data packages without active compensation. The solution is pre-knowledge of the approximate clock skew to narrow down the search window - ideally there will be just a single cross-correlation necessary to find the correlation peak. One option here is to calibrate the two involved clocks on high signal rates before applying the real link losses. By doing so, the signal to noise ratio increases and relaxes requirements for compensation, following in less computation efforts. Another option is to find clock skew some time before, where computation limits do not constrain. We found that measured clock skews from previous sessions work perfectly and allow us performing a single cross-correlation for recognizing the timing offset.

Systems with very high losses or accelerating clocks suffer from increased synchronization jitters during communication. Low number of correlation events reduce the precision of the correlation peak location by $1/\sqrt{N}$, following in bigger uncertainty of the estimated instantaneous skew during drift live correction. The stability of clocks impacts the overall synchronization performance as well, as the clock skew will have changed again during acquisition time without correction. Larger feedback loop times for compensa-

tion reduces peak location errors, but also increases the risk of potentially undetected skew from clock drifts. High precision clocks, like Rubidium oscillators, clearly have an advantage here that allow for much lower synchronization jitters < 1 ps during communication sessions, due to low drifts through high stability. Apart from signal to noise ratio and clock stability is the third factor for high synchronization performance the detector jitter. The correlation peak location is calculated with accuracy proportional to the detector jitter and hence also scales uncertainty of the estimated instantaneous skew. Particularly, high loss scenarios benefit from low detection jitters. We demonstrated that even 36 correlation events in 100 ms data packages are sufficient for synchronization jitter of a few tens of picosecond. The event rates are comparable to extremely high loss scenarios [21] (Table Id), but are enough to enable correlation peak tracking and keep the system locked. As nanowire detectors already have timing jitters of as low as tens of picosecond, synchronization performance with correlated photons will only increase in future.

To set our approach into broader perspective, we also shortly discuss limits with moving objects, like satellite[14, 15] or emerging drone-based [57, 58] quantum communication. Satellites introduce an effective clock skew, due to the Doppler effect caused by varying distance to the observer. At the smallest distance is the clock skew zero and may increase to a maximum of 20 μ s/s over a time scale of 6 min for low earth orbit satellites[59]. Whereas the maximum clock skew is comparable to our crystal oscillators, the clock acceleration $\partial(\Delta u)/\partial t$ is orders of magnitude bigger and amounts to approximately 55 ns/s². Thus, it is desirable to reduce the feedback and acquisition time to 100 ms or smaller that could result in clock drift jitters of 265 ps. However, with only a few correlation events per second[14, 60] available, it is impossible to choose acquisition times < 1 second. Ignoring noise, the absolute minimum would be to find at least a two correlation events. In conclusion, it is hardly feasible to correct for clock drifts without knowledge of the satellite's orbit. Drones move much slower than satellites and may be suited for synchronization – at least classically[61]. The speed is up to 30 m/s, introducing clock skews of up to 100 ns/s, being much smaller than the clock skew of our crystal oscillators. The main concern is acceleration of the drone, reaching up to 7 g (gravitational constant) and translating to 228 ns/s² clock drift. Sufficient kcps coincidence rates[57], in contrast to satellite links, give opportunity to select short feedback cycles for compensation of high drifts during drone acceleration. With small feedback loops and enough signal, correlated photons open doors for live remote detection of ve-

locity and acceleration of moving objects.

Correlated photons come with quantum communication systems naturally and are easy to recycle for high performance synchronization down to a few tens of picoseconds. Todays point-to-point or lab-to-lab communication sessions will be integrated in a network with multi-users tomorrow, as can be found in action already [10]. The networks are characterized by high scalability, integration and less resources, where highly stable but bulky clocks may not be desired. Where correlated photons used to be inappropriate for synchronizing clocks with high skew and strong drifts[42], we showed stable operation by new synchronization methods. Clock skew compensation and correlation peak live tracking allows for a wider range of use cases - especially in terms of scalability. Resistance to high losses, as would be common to large networks, still enables synchronization jitters < 50 ps and presents feasibility for application in real-life communication scenarios. Single photons are not copyable and bit-errors during communication are easy to detect due to the quantum origin of the single photon detection events [6, 7], indicating furthermore the potential for quantum secured time transfer [51, 52, 62].

ACKNOWLEDGMENTS

This research was conducted within the scope of the project QuNET, funded by the German Federal Ministry of Education and Research (BMBF) in the context of the federal government's research framework in IT-security "Digital. Secure. Sovereign.". The authors thank the whole QuNET team for helpful discussions and support in the development of sub-systems used in the experiment.

AUTHOR CONTRIBUTIONS

C.S. designed and performed the experiments. S.T. and S.S. developed essential hardware and software components with support from D.R.: S.S. developed the entanglement source. C.S. wrote the main part of the Python processing script with assistance from S.T.. F.S. proposed and directed the research. The first draft of the manuscript was written by C.S., F.S. and D.R. with assistance by M.C.P.. All authors discussed the results and reviewed the manuscript.

COMPETING INTERESTS STATEMENT

The authors declare no competing interest.

IV. METHODS

A. Theory

1. Description of total system jitter

The total system jitter of a quantum communication system determines the overall performance, from signal to noise ratio to secure bit rates. The total jitter can be easily calculated analytically by knowledge of the clock skew. Here we provide important scaling laws to estimate final signal to noise ratios, like significance or coincidence to accidentals ratio. As all jitter contributions originate from a random source, we consider a Gaussian function with RMS jitter σ that is normalized to have an area of 1,

$$g(t) = \frac{1}{\sqrt{2\pi\sigma^2}} \exp\left(-\frac{t^2}{2\sigma^2}\right). \quad (3)$$

The total jitter,

$$\sigma = \sqrt{\sigma_{\text{coh}}^2 + \sigma_{\text{tt}}^2 + \sigma_{\text{det}}^2 + \sigma_{\text{sync}}^2}, \quad (4)$$

reduces to,

$$\sigma \approx \sqrt{\sigma_{\text{det}}^2 + \sigma_{\text{sync}}^2}, \quad (5)$$

as the jitter contribution from the time tagger and coherence time is much smaller than the detector jitter. After a few steps of editing, we get

$$\sigma = \sigma_{\text{det}} \sqrt{1 + \frac{\sigma_{\text{sync}}^2}{\sigma_{\text{det}}^2}}, \quad (6)$$

giving the simulated jitter curves in Fig. 1e ($\sigma_{\text{det}} \approx 2800$ ps) and 1c ($\sigma_{\text{det}} \approx 300$ ps). The highest correlation peak value P_0 , given by the detector jitter σ_{det} , reduces, due to stronger synchronization jitter,

$$\frac{P}{P_0} = \frac{\sqrt{2\pi}\sigma_{\text{det}}}{\sqrt{2\pi}\sigma}. \quad (7)$$

With equation 5 it becomes,

$$P = \frac{P_0}{\sqrt{1 + \frac{\sigma_{\text{sync}}^2}{\sigma_{\text{det}}^2}}}, \quad (8)$$

providing the analytical trend in Fig. 1e ($\sigma_{\text{det}} \approx 2800$ ps) and 3c ($\sigma_{\text{det}} \approx 300$ ps).

The maximum coincidence to accidentals ratio CAR₀ in Fig. 3c has been simulated with

$$P_0 = \frac{r_C}{2r_A r_B}. \quad (9)$$

The maximum significance in Fig. 1e was gained from true experimental counts over equation[42],

$$\Delta u_{\text{max}} = \frac{r_C}{r_A r_B S_{\text{th}}}, \quad (10)$$

with $R_A = 240$ kHz, $R_B = 232$ kHz, $R_C = 7$ kHz and smallest step size in the clock skew search window of $\Delta u = 25$ ns/s.

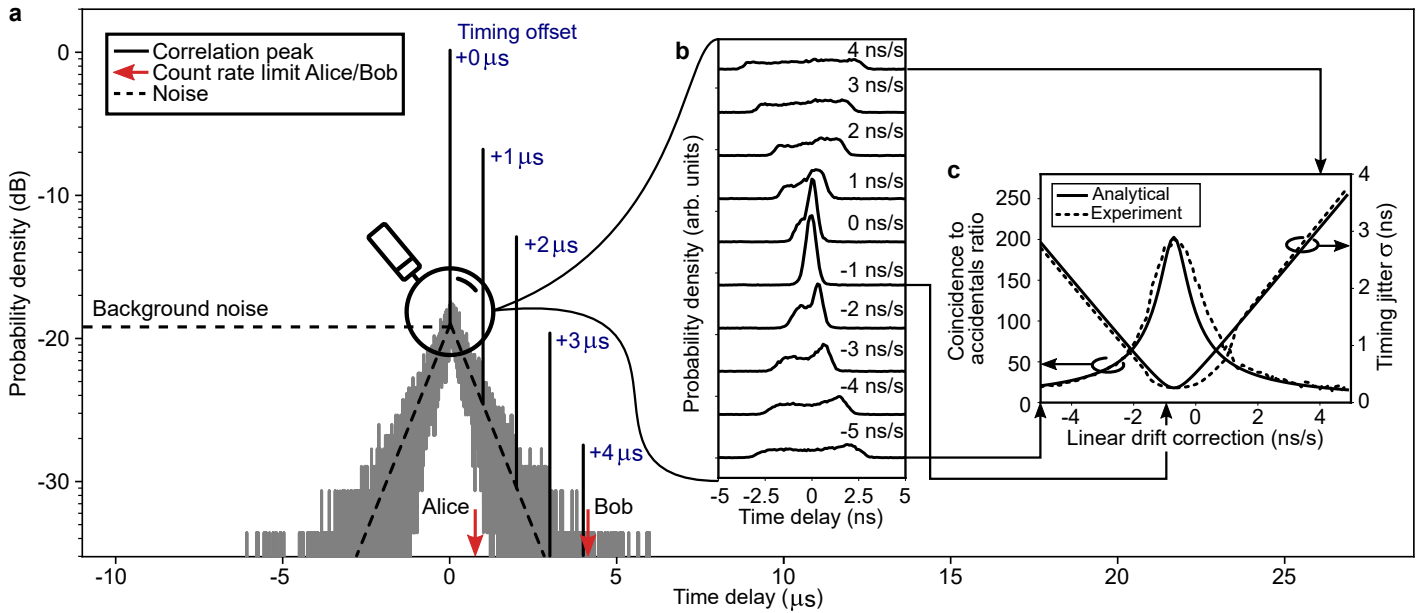


FIG. 3. **Fine tuning of clock skew through cross-correlation with Start-Stop method** **a** Correlation peaks for various timing offset accuracy. The noise values are highest at small time delay with -20 dB and reduce exponentially until approximately the inverse count rate at Bob is reached. For bad timing offset precision $> 2.5 \mu\text{s}$ is the peak noise level larger than the correlation peak. Peak search algorithms may still recover the peak here, instead of simple search of maximum at timing offset precisions $< 2.5 \mu\text{s}$. **b** Magnified view of timing offset corrected cross-correlation peaks for various clock skew compensation values. The shape of correlation peaks depends on the compensated clock skew and may be asymmetrical from clock instabilities. **c** The correlation peak coincidence to accidentals ratio (CAR) or width is ideal indicator for optimum clock skew compensation, as they become maximum and minimum, respectively.

2. Achievable jitter during live correction

The final synchronization jitter after live correction during a communication session is decided by clock drift and number of correlation events. Here we present analytical estimations of the synchronization limits that might be helpful for easy transfer to any communication scenario. The most important parameter is the instantaneous clock skew during a communication session. If it is nonzero, due to insufficient correction, the synchronization jitter will be nonzero. The clock skew derives from two or more detected peak locations τ_1 and τ_2 with temporal separation of T_{meas} ,

$$\Delta u = \frac{\tau_2 - \tau_1}{T_{\text{meas}}}. \quad (11)$$

However, low number of N correlation events give rise to an uncertainty of the correlation peak location $\delta\tau$ [42],

$$\delta\tau = \frac{\sigma}{\sqrt{N-1}}. \quad (12)$$

Via error propagation, we get the uncertainty of the clock skew,

$$\Delta u_{\text{meas}} = \sqrt{2} \frac{\delta\tau}{T_{\text{meas}}}. \quad (13)$$

Together with equations 1 and 12, coincidence rate r_C and acquisition time T_A is the synchronization jitter due to uncertainty from peak position measurement,

$$\sigma_{\text{meas}} = \frac{1}{2} \sqrt{2} \frac{\sigma}{\sqrt{r_C T_A - 1} T_{\text{meas}}} T_A. \quad (14)$$

The second jitter contribution comes from the clock drift $\partial(\Delta u)/\partial t$. Clock skew, that has not been foreseen previously, may accumulate over the feedback loop time T_{feed} ,

$$\Delta u_{\text{drift}} = \frac{\partial(\Delta u)}{\partial t} T_{\text{feed}}. \quad (15)$$

The resulting synchronization jitter, due to the drifting clocks, derives with equation 1 to,

$$\sigma_{\text{drift}} = \frac{1}{2} \frac{\partial(\Delta u)}{\partial t} T_{\text{feed}} T_A. \quad (16)$$

Both, measurement and synchronization jitter limit the total achievable synchronization jitter during live tracking,

$$\sigma_{\text{sync}}^2 = \sigma_{\text{meas}}^2 + \sigma_{\text{drift}}^2. \quad (17)$$

B. Clock skew fine tuning

Only careful fine tuning of the compensation clock skew to precision's much smaller than the estimated coarse skew reduces the synchronization jitter to minimum, due to its strong impact scaled through the acquisition time. As the timing offset is calculated with nanosecond accuracy in synchronization step 2, it is feasible to shrink down the observation window to $< 100 \text{ ns}$ to reduce computation efforts. Cross-correlations are now derived by the computation-efficient Start-Stop method [54–56]. In contrast to the FFT cross-correlation that correlates all timetags from Alice with all Bob timetags from Bob, the Start-Stop method calculates time differences between neighboring timetags. If

the timing offset was not calculated with precision smaller than $\text{Min}\{1/r_A, 1/r_B\}$, it rises the probability of wrongly calculated time differences and thus reduces the number of correlation events. The correlation peak height reduces and finally becomes smaller than the peak noise values (Fig. 3a). By compensation of the residual clock skew will the correlation peak compress to the smallest width $\sigma_{\text{min}} = 258 \text{ ps}$. In addition will the coincidence to accidentals ratio maximize at $\text{CAR}_0 = 204$ over a window determined by the total timing jitter. The experimental correlation peak is fit by a stretched Gaussian function and then the timing jitter derived from it. The experimental total jitter behaves perfectly as analytically given and the maximum peak scales according to a stretched Gaussian with same area (see Methods IV A 1). Clocks with high stability, i.e. a constant frequency difference between two clocks, create a jitter envelope with a plateau. Rubidium oscillators are known for their high stability of 10^{-12} over 1 second [63, 64] and create a jitter envelope with a plateau, as the frequency difference is almost constant over time. Quartz crystal oscillators on the other hand may show weak stability of only 10^{-11} to 10^{-9} over 1 second [45] that result in asymmetries and give rise to deviations between analytical and experimental trend in a region between -1 to 2 ns/s. The method for compensation of the clock skew by a simple peak search (Fig. 3c) may be done with arbitrary resolutions. Step sizes of $< 1 \text{ ns/s}$ work great to start live tracking of clock drifts in the last step of synchronization.

C. Correction of residual clock skew

Residual clock skews increase synchronization jitter and call for compensation during communication sessions. Fig. 4 represents the effect of correct compensation for Rubidium clocks. The correlation peak timing offset is tracked over n data points. Any change of timing offset would be caused by an instantaneous drift. Here the timing offset changes by approximately 8 ns in 1 minute. By taking the measured residual clock skew into account for the future feedback loop, we can reduce the timing offset change and subsequently the synchronization jitter. Long averaging times work especially well for highly stable clocks, as Rubidium clocks. The timing offset changes by less than 1.5 ns over 4 minutes after the first correction already, providing residual clock skews of $< 6.4 \text{ ps/s}$ and thus easily synchronization jitters $< 0.32 \text{ ps}$ in typical 100 ms data package sizes.

D. Photon pair rates

The experimentally detected photon pair rates determine achievable signal to noise ratios and limit the synchronization jitter under high losses. Figure 5 represents the rates from experiment (Fig. 2a,b). At one receiver is a polarization analysis module that projects the single photons on a state Horizontal, Vertical, Diagonal or Anti-Diagonal, where one channel will be used for time of arrival measurements and synchronization. The other receiver does not differentiate between polarizations. In consequence is 75 %

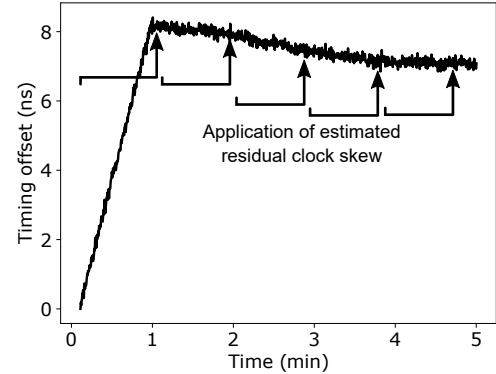


FIG. 4. Estimation of residual clock skew over a feedback time of approximately 1 minute with two Rubidium clocks. The residual clock skew over the last 4 minutes amounts to 6.4 ps/s , resulting in synchronization jitters of approximately 0.32 ps over acquisition time of 100 ms.

of single counts at the non-differentiating receiver not correlated, as the polarization does not match. From the correlation rate under the RMS window of 9 k/s and potentially correlated single counts of 50 k/s, we estimate the source to have heralding of around 18 %. Through a variable attenuator reduces the rates of correlation events down to less than 400 Hz. Synchronization tracking is feasible even under strong fluctuations of up to 20 % (RMS) and only 36 correlations events over the acquisition time of 100 ms.

E. Experimental clock drift

Knowledge of the clock stability provides important measures about the limiting synchronization jitters. To estimate the clock stability, we first compare the timing jitter without tracking to the reference (Fig. 2b). Any increase from the reference is caused by synchronization jitters through residual clock skews Δu (equation 1). The residual, not compensated clock skew is plotted in Fig. 6a and amounts to more than 10 ns/s. Almost ideal synchronization may be achieved if the residual clock skew was constant. However, crystal oscillators may have time-dependent frequencies that result in variation of the residual clock skew. Fig. 6b indicates acceleration of the clocks with time with mean value of zero and standard deviation of 320 ps/s^2 . High clock drifts require small feedback times for compensation that simultaneously demands many correlation events.

The time taggers are equipped with external crystal oscillators without temperature control. The data sheet accuracy is $\pm 20 \text{ ppm}$, aging $\pm 3 \text{ ppm/ first year}$, $\pm 1 \text{ ppm/year}$ and temperature dependence $\pm 0.125 \text{ ppm}$ ($25^\circ\text{C} \dots 85^\circ\text{C}$). The Rubidium clocks are temperature controlled with accuracy $\pm 10^{-4} \text{ ppm}$ (ambient temperature $0^\circ\text{C} \dots 40^\circ\text{C}$), aging $< 5 \times 10^{-5} \text{ ppm/month}$, stability over 1s is 10^{-5} ppm .

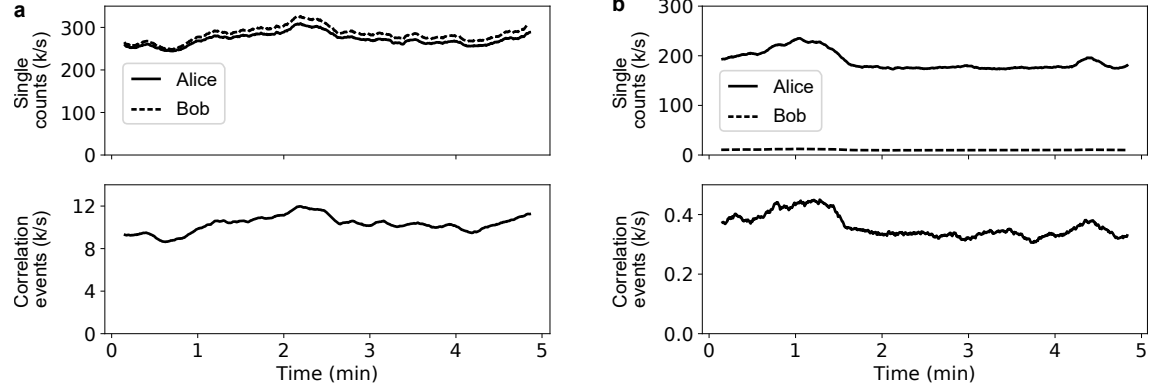


FIG. 5. Photon pair rate in low loss **a** and high loss **b** regime according to table I

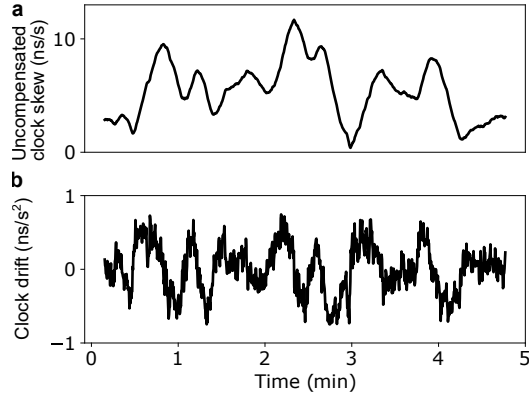


FIG. 6. **a** Uncompensated clock skew in high loss regime I. **b** The time dependent clock drift is zero on average with standard deviation of 320 ps/s^2 .

-
- [1] J. C. Bellamy. Digital network synchronization. *IEEE Communications Magazine*, 33(4):70–83, 1995.
- [2] Lakshay Narula and Todd E. Humphreys. Requirements for secure clock synchronization. *IEEE Journal of Selected Topics in Signal Processing*, 12(4):749–762, 2018.
- [3] A. G. Phadke, B. Pickett, M. Adamiak, M. Begovic, G. Benmouyal, R. O. Burnett, T. W. Cease, J. Goossens, D. J. Hansen, M. Kezunovic, L. L. Mankoff, P. G. McLaren, G. Michel, R. J. Murphy, J. Nordstrom, M. S. Sachdev, H. S. Smith, J. S. Thorp, M. Trotignon, T. C. Wang, and M. A. Xavier. Synchronized sampling and phasor measurements for relaying and control. *IEEE Transactions on Power Delivery*, 9(1):442–452, 1994.
- [4] James J. Angel*. When finance meets physics: The impact of the speed of light on financial markets and their regulation. *Financial Review*, 49(2):271–281, 2014.
- [5] James C. Corbett, Jeffrey Dean, Michael Epstein, Andrew Fikes, Christopher Frost, J. J. Furman, Sanjay Ghemawat, Andrey Gubarev, Christopher Heiser, Peter Hochschild, Wilson Hsieh, Sebastian Kanthak, Eugene Kogan, Hongyi Li, Alexander Lloyd, Sergey Melnik, David Mwaura, David Nagle, Sean Quinlan, Rajesh Rao, Lindsay Rolig, Yasushi Saito, Michal Szymaniak, Christopher Taylor, Ruth Wang, and Dale Woodford. Spanner: Google's globally distributed database. *ACM Trans. Comput. Syst.*, 31(3), 2013.
- [6] Charles H. Bennett and Gilles Brassard. Quantum cryptography: Public key distribution and coin tossing. *Theoretical Computer Science*, 560:7–11, 2014.
- [7] Artur K. Ekert. Quantum cryptography based on bell's theorem. *Physical review letters*, 67(6):661–663, 1991.
- [8] T. E. Northup and R. Blatt. Quantum information transfer using photons. *Nature Photonics*, 8(5):356–363, 2014.
- [9] Nicolas Gisin and Rob Thew. Quantum communication. *Nature Photonics*, 1(3):165–171, 2007.
- [10] Yu-Ao Chen, Qiang Zhang, Teng-Yun Chen, Wen-Qi Cai, Sheng-Kai Liao, Jun Zhang, Kai Chen, Juan Yin, Ji-Gang Ren, Zhu Chen, Sheng-Long Han, Qing Yu, Ken Liang, Fei Zhou, Xiao Yuan, Mei-Sheng Zhao, Tian-Yin Wang, Xiao Jiang, Liang Zhang, Wei-Yue Liu, Yang Li, Qi Shen, Yuan Cao, Chao-Yang Lu, Rong Shu, Jian-Yu Wang, Li Li, Nai-Le Liu, Feihu Xu, Xiang-Bin Wang, Cheng-Zhi Peng, and Jian-Wei Pan. An integrated space-to-ground quantum communication network over 4,600 kilometres. *Nature*, 589:214–219, 2021.
- [11] David L. Mills. *Computer network time synchronization: The Network Time Protocol on Earth and in space*. CRC Press, Boca Raton FL, 2nd ed. edition, 2011.
- [12] P. Berceau, M. Taylor, J. Kahn, and L. Hollberg. Space-

- time reference with an optical link. *Classical and Quantum Gravity*, 33(13):135007, 2016.
- [13] Akihisa Tomita, Ken-ichiro Yoshino, Yoshihiro Nambu, Akio Tajima, Akihiro Tanaka, Seigo Takahashi, Wakako Maeda, Shigehito Miki, Zhen Wang, Mikio Fujiwara, and Masahide Sasaki. High speed quantum key distribution system. *Optical Fiber Technology*, 16(1):55–62, 2010.
- [14] Juan Yin, Yu-Huai Li, Sheng-Kai Liao, Meng Yang, Yuan Cao, Liang Zhang, Ji-Gang Ren, Wen-Qi Cai, Wei-Yue Liu, Shuang-Lin Li, Rong Shu, Yong-Mei Huang, Lei Deng, Li Li, Qiang Zhang, Nai-Le Liu, Yu-Ao Chen, Chao-Yang Lu, Xiang-Bin Wang, Feihu Xu, Jian-Yu Wang, Cheng-Zhi Peng, Artur K. Ekert, and Jian-Wei Pan. Entanglement-based secure quantum cryptography over 1,120 kilometres. *Nature*, 582(7813):501–505, 2020.
- [15] Sheng-Kai Liao, Wen-Qi Cai, Wei-Yue Liu, Liang Zhang, Yang Li, Ji-Gang Ren, Juan Yin, Qi Shen, Yuan Cao, Zheng-Ping Li, Feng-Zhi Li, Xia-Wei Chen, Li-Hua Sun, Jian-Jun Jia, Jin-Cai Wu, Xiao-Jun Jiang, Jian-Feng Wang, Yong-Mei Huang, Qiang Wang, Yi-Lin Zhou, Lei Deng, Tao Xi, Lu Ma, Tai Hu, Qiang Zhang, Yu-Ao Chen, Nai-Le Liu, Xiang-Bin Wang, Zhen-Cai Zhu, Chao-Yang Lu, Rong Shu, Cheng-Zhi Peng, Jian-Yu Wang, and Jian-Wei Pan. Satellite-to-ground quantum key distribution. *Nature*, 549(7670):43–47, 2017.
- [16] Sören Wengerowsky, Siddarth Koduru Joshi, Fabian Steinlechner, Julien R. Zichi, Bo Liu, Thomas Scheidl, Sergiy M. Dobrovolskiy, René van der Molen, Johannes W. N. Los, Val Zwiller, Marijn A. M. Versteegh, Alberto Mura, Davide Calonico, Massimo Inguscio, Anton Zeilinger, André Xuereb, and Rupert Ursin. Passively stable distribution of polarisation entanglement over 192 km of deployed optical fibre. *npj Quantum Information*, 6(1):012307, 2020.
- [17] Ivan Marcikic, Antía Lamas-Linares, and Christian Kurtsiefer. Free-space quantum key distribution with entangled photons. *Applied Physics Letters*, 89(10):101122, 2006.
- [18] Fabian Steinlechner, Sebastian Ecker, Matthias Fink, Bo Liu, Jessica Bavaresco, Marcus Huber, Thomas Scheidl, and Rupert Ursin. Distribution of high-dimensional entanglement via an intra-city free-space link. *Nature communications*, 8:15971, 2017.
- [19] Yicheng Shi, Soe Moe Thar, Hou Shun Poh, James A. Grieve, Christian Kurtsiefer, and Alexander Ling. Stable polarization entanglement based quantum key distribution over a deployed metropolitan fiber. *Applied Physics Letters*, 117(12):124002, 2020.
- [20] R. Ursin, F. Tiefenbacher, T. Schmitt-Manderbach, H. Weier, T. Scheidl, M. Lindenthal, B. Blauensteiner, T. Jennewein, J. Perdigues, P. Trojek, B. Ömer, M. Fürst, M. Meyenburg, J. Rarity, Z. Sodnik, C. Barbieri, H. Weinfurter, and A. Zeilinger. Entanglement-based quantum communication over 144 km. *Nature Physics*, 3(7):481–486, 2007.
- [21] Sebastian Ecker, Bo Liu, Johannes Handsteiner, Matthias Fink, Dominik Rauch, Fabian Steinlechner, Thomas Scheidl, Anton Zeilinger, and Rupert Ursin. Strategies for achieving high key rates in satellite-based qkd. *npj Quantum Information*, 7(1), 2021.
- [22] Erik F. Dierikx, Anders E. Wallin, Thomas Fordell, Jani Myyry, Petri Koponen, Mikko Merimaa, Tjeerd J. Pinkert, Jeroen C. J. Koelemeij, Henk Z. Peek, and Rob Smets. White rabbit precision time protocol on long-distance fiber links. *IEEE transactions on ultrasonics, ferroelectrics, and frequency control*, 63(7):945–952, 2016.
- [23] Michael Wahl, Tino Röhlicke, Sebastian Kulisch, Sumeet Rohilla, Benedikt Krämer, and Andreas C. Hocke. Photon arrival time tagging with many channels, sub-nanosecond deadtime, very high throughput, and fiber optic remote synchronization. *The Review of scientific instruments*, 91(1):013108, 2020.
- [24] Eleni Diamanti, Hoi-Kwong Lo, Bing Qi, and Zhiliang Yuan. Practical challenges in quantum key distribution. *npj Quantum Information*, 2(1):16025, 2016.
- [25] Daniel K. L. Oi, Alex Ling, Giuseppe Vallone, Paolo Villoresi, Steve Greenland, Emma Kerr, Malcolm Macdonald, Harald Weinfurter, Hans Kuiper, Edoardo Charbon, and Rupert Ursin. Cubesat quantum communications mission. *EPJ Quantum Technology*, 4(1), 2017.
- [26] Erik Kerstel, Arnaud Gardelein, Mathieu Barthelemy, Matthias Fink, Siddarth Koduru Joshi, Rupert Ursin, and The CSUG Team. Nanobob: a cubesat mission concept for quantum communication experiments in an uplink configuration. *EPJ Quantum Technology*, 5(1):6, 2018.
- [27] Ji-Gang Ren, Ping Xu, Hai-Lin Yong, Liang Zhang, Sheng-Kai Liao, Juan Yin, Wei-Yue Liu, Wen-Qi Cai, Meng Yang, Li Li, Kui-Xing Yang, Xuan Han, Yong-Qiang Yao, Ji Li, Hai-Yan Wu, Song Wan, Lei Liu, Ding-Quan Liu, Yao-Wu Kuang, Zhi-Ping He, Peng Shang, Cheng Guo, Ru-Hua Zheng, Kai Tian, Zhen-Cai Zhu, Nai-Le Liu, Chao-Yang Lu, Rong Shu, Yu-Ao Chen, Cheng-Zhi Peng, Jian-Yu Wang, and Jian-Wei Pan. Ground-to-satellite quantum teleportation. *Nature*, 549(7670):70–73, 2017.
- [28] Raju Valivarthi, Marcel.li Grima Puigibert, Qiang Zhou, Gabriel H. Aguilar, Varun B. Verma, Francesco Marsili, Matthew D. Shaw, Sae Woo Nam, Daniel Oblak, and Wolfgang Tittel. Quantum teleportation across a metropolitan fibre network. *Nature Photonics*, 10(10):676–680, 2016.
- [29] Yoshiaki Tsujimoto, Motoki Tanaka, Nobuo Iwasaki, Rikizo Ikuta, Shigehito Miki, Taro Yamashita, Hirotaka Terai, Takashi Yamamoto, Masato Koashi, and Nobuyuki Imoto. High-fidelity entanglement swapping and generation of three-qubit ghz state using asynchronous telecom photon pair sources. *Scientific reports*, 8(1):1446, 2018.
- [30] Jian-Wei Pan, Dik Bouwmeester, Harald Weinfurter, and Anton Zeilinger. Experimental entanglement swapping: Entangling photons that never interacted. *Physical Review Letters*, 80(18):3891–3894, 1998.
- [31] Richard Jozsa, Daniel S. Abrams, Jonathan P. Dowling, and Colin P. Williams. Quantum clock synchronization based on shared prior entanglement. *Physical Review Letters*, 85(9):2010–2013, 2000.
- [32] Isaac L. Chuang. Quantum algorithm for distributed clock synchronization. *Physical Review Letters*, 85(9):2006–2009, 2000.
- [33] V. Giovannetti, S. Lloyd, L. Maccone, and F. N. Wong. Clock synchronization with dispersion cancellation. *Physical review letters*, 87(11):117902, 2001.
- [34] Marko Krčo and Prabasaj Paul. Quantum clock synchronization: Multiparty protocol. *Physical Review A*, 66(2), 2002.
- [35] Xiangyu Kong, Tao Xin, Shi-Jie Wei, Bixue Wang, Yunzhao Wang, Keren Li, and Gui-Lu Long. Demonstration of multiparty quantum clock synchronization. *Quantum Information Processing*, 17(11), 2018.
- [36] Vittorio Giovannetti, Seth Lloyd, and Lorenzo Maccone. Quantum-enhanced positioning and clock synchronization. *Nature*, 412(6845):417–419, 2001.
- [37] Runai Quan, Ruifang Dong, Xiao Xiang, Baihong Li, Tao Liu, and Shougang Zhang. High-precision nonlocal temporal correlation identification of entangled photon pairs for quantum clock synchronization. *The Review of scientific instruments*, 91(12):123109, 2020.
- [38] Runai Quan, Yiwei Zhai, Mengmeng Wang, Feiyan Hou, Shaofeng Wang, Xiao Xiang, Tao Liu, Shougang Zhang,

- and Ruifang Dong. Demonstration of quantum synchronization based on second-order quantum coherence of entangled photons. *Scientific reports*, 6:30453, 2016.
- [39] Runai Quan, Ruifang Dong, Yiwei Zhai, Feiyan Hou, Xiao Xiang, Hui Zhou, Chaolin Lv, Zhen Wang, Lixing You, Tao Liu, and Shougang Zhang. Simulation and realization of a second-order quantum-interference-based quantum clock synchronization at the femtosecond level. *Optics letters*, 44(3):614–617, 2019.
- [40] Virginia D'Auria, Bruno Fedrici, Lutfi Arif Ngah, Florian Kaiser, Laurent Labonté, Olivier Alibart, and Sébastien Tanzilli. A universal, plug-and-play synchronisation scheme for practical quantum networks. *npj Quantum Information*, 6(1):1023, 2020.
- [41] Alejandra Valencia, Giuliano Scarcelli, and Yanhua Shih. Distant clock synchronization using entangled photon pairs. *Applied Physics Letters*, 85(13):2655–2657, 2004.
- [42] Caleb Ho, Antía Lamas-Linares, and Christian Kurtsiefer. Clock synchronization by remote detection of correlated photon pairs. *New Journal of Physics*, 11(4):045011, 2009.
- [43] Yin-Ping Yao, Tong-Yi Zhang, Ren-Gang Wan, and Wei Zhao. Review on quantum clock synchronization schemes. In Pierre Galarneau, Xu Liu, and Pengcheng Li, editors, *Photonics and Optoelectronics Meetings (POEM) 2011: Optoelectronic Sensing and Imaging*, SPIE Proceedings, page 833202. SPIE, 2012.
- [44] Jianwei Lee, Lijiong Shen, Alessandro Cerè, James Troupe, Antia Lamas-Linares, and Christian Kurtsiefer. Symmetrical clock synchronization with time-correlated photon pairs. *Applied Physics Letters*, 114(10):101102, 2019.
- [45] Francisco Tirado-Andrés and Alvaro Araujo. Performance of clock sources and their influence on time synchronization in wireless sensor networks. *International Journal of Distributed Sensor Networks*, 15(9):155014771987937, 2019.
- [46] S. Bregni. Clock stability characterization and measurement in telecommunications. *IEEE Transactions on Instrumentation and Measurement*, 46(6):1284–1294, 1997.
- [47] Costantino Agnesi, Marco Avanesi, Luca Calderaro, Andrea Stanco, Giulio Foletto, Mujtaba Zahidy, Alessia Scriminich, Francesco Vedovato, Giuseppe Vallone, and Paolo Villoresi. Simple quantum key distribution with qubit-based synchronization and a self-compensating polarization encoder. *Optica*, 7(4):284–290, 2020.
- [48] Luca Calderaro, Andrea Stanco, Costantino Agnesi, Marco Avanesi, Daniele Dequal, Paolo Villoresi, and Giuseppe Vallone. Fast and simple qubit-based synchronization for quantum key distribution. *Physical Review Applied*, 13(5), 2020.
- [49] James Williams, Martin Suchara, Tian Zhong, Hong Qiao, Rajkumar Kettimuthu, and Riku Fukumori. Implementation of quantum key distribution and quantum clock synchronization via time bin encoding. In Philip R. Hemmer and Alan L. Migdall, editors, *Quantum Computing, Communication, and Simulation*, page 5. SPIE, 06.03.2021 - 12.03.2021.
- [50] P. Kómár, E. M. Kessler, M. Bishof, L. Jiang, A. S. Sørensen, J. Ye, and M. D. Lukin. A quantum network of clocks. *Nature Physics*, 10(8):582–587, 2014.
- [51] Hui Dai, Qi Shen, Chao-Ze Wang, Shuang-Lin Li, Wei-Yue Liu, Wen-Qi Cai, Sheng-Kai Liao, Ji-Gang Ren, Juan Yin, Yu-Ao Chen, Qiang Zhang, Feihu Xu, Cheng-Zhi Peng, and Jian-Wei Pan. Towards satellite-based quantum-secure time transfer. *Nature Physics*, 11:25, 2020.
- [52] Jianwei Lee, Lijiong Shen, Alessandro Cerè, James Troupe, Antia Lamas-Linares, and Christian Kurtsiefer. Asymmetric delay attack on an entanglement-based bidirectional clock synchronization protocol. *Applied Physics Letters*, 115(14):141101, 2019.
- [53] Matthäus Halder, Alexios Beveratos, Robert T. Thew, Corentin Jorel, Hugo Zbinden, and Nicolas Gisin. High coherence photon pair source for quantum communication. *New Journal of Physics*, 10(2):023027, 2008.
- [54] Christian Brunel, Brahim Lounis, Philippe Tamarat, and Michel Orrit. Triggered source of single photons based on controlled single molecule fluorescence. *Physical Review Letters*, 83(14):2722–2725, 1999.
- [55] R. Alléaume, F. Treussart, J-M Courty, and J-F Roch. Photon statistics characterization of a single-photon source. *New Journal of Physics*, 6:85, 2004.
- [56] L. J. Martínez, T. Pelini, V. Waselowski, J. R. Maze, B. Gil, G. Cassabois, and V. Jacques. Efficient single photon emission from a high-purity hexagonal boron nitride crystal. *Physical Review B*, 94(12), 2016.
- [57] Samantha Isaac, Andrew Conrad, Alex Hill, Kyle Herndon, Brian Wilens, Dalton Chaffee, Daniel Sanchez-Rosales, Roderick Cochran, Daniel Gauthier, and Paul Kwiat. Drone-based quantum key distribution. In *Conference on Lasers and Electro-Optics*, page JW2A.16. Optical Society of America, 2020.
- [58] Andrew Conrad, Samantha Isaac, Roderick Cochran, Daniel Sanchez-Rosales, Brian Wilens, Akash Gutha, Tahereh Rezaei, Dan Gauthier, and Paul Kwiat. Drone-based quantum key distribution: Qkd. In Hamid Hemmati and Don M. Boroson, editors, *Free-Space Laser Communications XXXIII*, page 29. SPIE, 06.03.2021 - 12.03.2021.
- [59] I. Ali, N. Al-Dhahir, and J. E. Hershey. Doppler characterization for leo satellites. *IEEE Transactions on Communications*, 46(3):309–313, 1998.
- [60] Juan Yin, Yuan Cao, Yu-Huai Li, Sheng-Kai Liao, Liang Zhang, Ji-Gang Ren, Wen-Qi Cai, Wei-Yue Liu, Bo Li, Hui Dai, Guang-Bing Li, Qi-Ming Lu, Yun-Hong Gong, Yu Xu, Shuang-Lin Li, Feng-Zhi Li, Ya-Yun Yin, Zi-Qing Jiang, Ming Li, Jian-Jun Jia, Ge Ren, Dong He, Yi-Lin Zhou, Xiao-Xiang Zhang, Na Wang, Xiang Chang, Zhen-Cai Zhu, Nai-Le Liu, Yu-Ao Chen, Chao-Yang Lu, Rong Shu, Cheng-Zhi Peng, Jian-Yu Wang, and Jian-Wei Pan. Satellite-based entanglement distribution over 1200 kilometers. *Science*, 356(6343):1140–1144, 2017.
- [61] Hugo Bergeron, Laura C. Sinclair, William C. Swann, Isaac Khader, Kevin C. Cossel, Michael Cermak, Jean-Daniel Deschênes, and Nathan R. Newbury. Femtosecond time synchronization of optical clocks off of a flying quadcopter. *Nature communications*, 10(1):1819, 2019.
- [62] James Troupe and Antia Lamas-Linares. Secure quantum clock synchronization. In Zameer U. Hasan, Philip R. Hemmer, Alan L. Migdall, and Alan E. Craig, editors, *Advances in Photonics of Quantum Computing, Memory, and Communication XI*, page 20. SPIE, 27.01.2018 - 01.02.2018.
- [63] Jacques Vanier and Laurent-Guy Bernier. On the signal-to-noise ratio and short-term stability of passive rubidium frequency standards. *IEEE Transactions on Instrumentation and Measurement*, IM-30(4):277–282, 1981.
- [64] B. M. Penrod. Adaptive temperature compensation of gps disciplined quartz and rubidium oscillators. In *Proceedings of 1996 IEEE International Frequency Control Symposium*, pages 980–987, 1996.